

# An observational test for correlations between cosmic rays and magnetic fields

Rodion Stepanov<sup>2,3\*</sup>, Anvar Shukurov<sup>1</sup>, Andrew Fletcher<sup>1,4</sup>, Rainer Beck<sup>4</sup>,  
Laura La Porta<sup>4</sup>, Fatemeh Tabatabaei<sup>5</sup>

<sup>1</sup>*School of Mathematics and Statistics, Newcastle University, Newcastle upon Tyne, NE1 7RU, UK*

<sup>2</sup>*Institute of Continuous Media Mechanics, Academy of Sciences, 1 Korolyov St., Perm 614013, Russia*

<sup>3</sup>*Department of Applied Mathematics and Mechanics, National Research Polytechnic University of Perm, 29 Komsomolskii Av., 614990, Perm, Russia*

<sup>4</sup>*Max-Planck Institut für Radioastronomie, Auf dem Hügel 69, Bonn D-53121, Germany*

<sup>5</sup>*Max Planck Institut für Astronomie, Königstuhl 17, Heidelberg D-69117, Germany*

Accepted .... Received ....; in original form ...

## ABSTRACT

We derive the magnitude of fluctuations in total synchrotron intensity in the Milky Way, both from observations and from theory under various assumption about the relation between cosmic rays and interstellar magnetic fields. Given the relative magnitude of the fluctuations in the Galactic magnetic field suggested by the Faraday rotation and polarization data, the observations are inconsistent with local energy equipartition between cosmic rays and magnetic fields. Our analysis of synchrotron fluctuations suggests that the distribution of cosmic rays is nearly uniform at scales of order 100 pc, in contrast to that of the interstellar magnetic field. A conservative upper limit on the relative variations in the cosmic ray number density is 0.2–0.4 at the scales of order 100 pc. Our results are consistent with a mild anticorrelation between cosmic-ray and magnetic energy densities at these scales. Energy equipartition between cosmic rays and magnetic fields still may hold, but at scales exceeding 1 kpc.

**Key words:** cosmic rays – magnetic fields – galaxies: ISM – galaxies: magnetic fields – radio continuum: galaxies – radio continuum: general

## 1 MOTIVATION AND BACKGROUND

The concept of energy equipartition between cosmic rays and magnetic fields and similar assumptions such as pressure equality (Longair 1994; Beck & Krause 2005; Arbutina et al. 2012) are often used in the analysis and interpretation of radio astronomical observations. This idea was originally suggested in order to estimate, from a measurement of the synchrotron brightness of a radio source, the magnetic field and cosmic ray energies of the source *as a whole* (Burbidge 1956b,a). A physically attractive feature of the equipartition state is that it approximately minimizes the total energy of the radio source.

The energy density of cosmic rays is mainly determined by their proton component, whereas the synchrotron intensity depends on the number density of relativistic electrons. Therefore, in order to estimate magnetic field energy, an assumption needs to be made about the ratio of the energy densities of the relativistic protons and electrons; the often adopted value for this ratio is 100, as suggested by the Milky Way data (Beck & Krause 2005). This ratio is adopted

to be unity in applications to galaxy clusters, radio galaxies and active objects (Carilli & Taylor 2002).

However, more recently this concept has been extended to large-scale trends in synchrotron intensity and to local energy densities at sub-kiloparsec scales in well-resolved radio sources, such as spiral galaxies (e.g., Beck et al. 2005; Beck 2007; Chyży 2008; Tabatabaei et al. 2008; Fletcher et al. 2011). Another important application of the equipartition hypothesis, first suggested by Parker (1966, 1969, 1979), is to the hydrostatic equilibrium of the interstellar gas. Here magnetic and cosmic ray pressures are assumed to be in a constant ratio, in practice taken to be unity. This application appeals to equipartition (or, more precisely, pressure equality) at larger scales of the order of kiloparsec. The spatial relation between fluctuations in magnetic field and cosmic rays is crucial for a proposed method to measure magnetic helicity in the ISM (Oppermann et al. 2011) (see also Volegova & Stepanov 2010).

The physical basis of the equipartition assumption remains elusive. Since cosmic rays are confined within a radio source by magnetic fields, it seems natural to expect that the two energy densities are somehow related: if the magnetic field energy density  $\epsilon_B$  is smaller than that of the cosmic rays,  $\epsilon_{cr}$ , the cosmic rays would be able to ‘break through’ the magnetic field and escape; whereas a larger magnetic energy density would result in the accumula-

\* E-mail: rodion@icmm.ru (RS); anvar.shukurov@ncl.ac.uk (AS); andrew.fletcher@ncl.ac.uk (AF); rbeck@mpifr-bonn.mpg.de (RB); laporta@mpifr-bonn.mpg.de (LLP); taba@mpia.de (FT)

tion of cosmic rays. Thus, the system is likely to be self-regulated to energy equipartition,  $\epsilon_B \approx \epsilon_{\text{cr}}$ . A slightly different version of these arguments refers to the equality of the two pressures,<sup>1</sup> giving  $\epsilon_B \approx \frac{1}{3}\epsilon_{\text{cr}}$ .

However plausible one finds these arguments, it is difficult to substantiate them. In particular, models of cosmic ray confinement suggest that the cosmic ray diffusion tensor depends on the *ratio*  $(\delta B/B_0)^2$ , where  $\delta B$  is the magnitude of magnetic field fluctuations at a scale equal to the proton gyroradius and  $B_0$  is the mean magnetic field (e.g., Berezhinskii et al. 1990). The magnetic field strength can determine the streaming velocity of cosmic rays via the Alfvén speed, but the theory of cosmic ray propagation and confinement relates  $\epsilon_{\text{cr}}$  to the intensity of cosmic ray sources rather than to the local magnetic field strength. Despite their uncertain basis, equipartition arguments remain popular as they provide ‘reasonable’ estimates of magnetic fields in radio sources, and also because they often offer the only practical way to obtain such estimates.

Equipartition between cosmic rays and magnetic fields can rarely be tested observationally. Chi & Wolfendale (1993) used  $\gamma$ -ray observations of the Magellanic clouds to calculate the energy density of cosmic rays independently of the equipartition assumption. They further calculated magnetic energy density from radio continuum data at a wavelength of about  $\lambda 12$  cm. The resulting magnetic energy density is two orders of magnitude larger than that of cosmic rays, and Chi & Wolfendale (1993) argue that the discrepancy cannot be removed by assuming a proton-to-electron ratio for cosmic rays different from the standard value of 100 (see, however, Pohl 1993).

An independent estimate of magnetic field strength can be obtained for synchrotron sources of high surface brightness (e.g., active galactic nuclei) where the relativistic plasma absorbs an observable lower-frequency part of the radio emission (synchrotron self-absorption). Then magnetic field strength can be estimated from the frequency, the flux density and the angular size of the synchrotron source at the turnover frequency (Sligh 1963; Williams 1963; Scheuer & Williams 1968). Scott & Readhead (1977) and Readhead (1994) concluded, from low-frequency observations of compact radio sources whose angular size can be determined from interplanetary scintillations, that there is no significant evidence of strong departures from equipartition. In the sources with strong synchrotron self-absorption in their sample, the total energy is within a factor of 10 above the minimum energy. Orienti & Dallacasa (2008) observed, using VLBI, five young, very compact radio sources to suggest that magnetic fields in them are quite close to the equipartition value. Physical conditions in spiral galaxies are quite different from those in compact, active radio sources, and departures from equipartition by a factor of several in terms of magnetic field strength would be quite significant in the context of spiral galaxies.

Here we test the equipartition hypothesis using another approach (see also Stepanov et al. 2009). We calculate the relative magnitude of fluctuations in synchrotron intensity using model random magnetic field and cosmic ray distributions with a prescribed degree of cross-correlations. When the results are compared with

observations, it becomes clear that local energy equipartition is implausible as it would produce stronger fluctuations of the synchrotron emissivity than are observed. Instead, the observed synchrotron fluctuations suggest weak variations in the cosmic ray number density or an anticorrelation between cosmic rays and magnetic fields, perhaps indicative of pressure equilibrium. We conclude that local energy equipartition is unlikely in spiral galaxies at the integral scale of the fluctuations, of order 100 pc. We discuss the dynamics of cosmic rays to argue in favour of equipartition at larger scales of order 1 kpc, comparable to the scale of the mean magnetic field and to the cosmic-ray diffusion scale.

## 2 THE MAGNITUDE OF FLUCTUATIONS IN INTERSTELLAR MAGNETIC FIELDS

Interstellar magnetic fields are turbulent, with the ratio of the random magnetic field to its mean component known from observations of Faraday rotation, independently of the equipartition assumption. Denoting the standard deviation of the turbulent magnetic field by  $\sigma_b^2 = \overline{B^2} - B_0^2$  and the mean field strength as  $B_0 = |\overline{\mathbf{B}}|$ , where bar denotes appropriate averaging (usually volume or line-of-sight averaging), the relative fluctuations in magnetic field strength in the Solar vicinity of the Milky Way is estimated as (Ruzmaikin et al. 1988; Ohno & Shibata 1993; Beck et al. 1996)

$$\delta_b^2 \equiv \left( \frac{\sigma_b}{B_0} \right)^2 \simeq 3\text{--}10. \quad (1)$$

Similar estimates result from radio observations of nearby spiral galaxies where the degree of polarization of the integrated emission at 4.8 GHz is a few per cent, with a range  $p \simeq 0.01\text{--}0.18$  (Stil et al. 2009). These data are affected by beam depolarization, so they only give upper limits for  $\delta_b^2$ . More typical values of the fractional polarisation in spiral galaxies are  $p = 0.01\text{--}0.05$  within spiral arms and 0.1 on average. The degree of polarization at short wavelengths where Faraday rotation is negligible can be estimated as (Burn 1966; Sokoloff et al. 1998)

$$p = p_0 \frac{B_{0\perp}^2}{B_{0\perp}^2 + \frac{2}{3}\sigma_b^2} \quad (2)$$

where  $B_{0\perp}$  is the strength of the large-scale magnetic field in the sky plane,  $p_0 \approx 0.75$ , and the random magnetic field is assumed to be isotropic,  $b_{\perp}^2 = \frac{2}{3}\sigma_b^2$ . This yields

$$\delta_b^2 \simeq \frac{3}{2} \left( \frac{p_0}{p} - 1 \right) \gtrsim 4 \quad \text{for } p < 0.2 \quad (3)$$

in a good agreement with the Milky Way data obtained from Faraday rotation measures. For  $p = 0.05\text{--}0.1$ , we obtain  $\delta_b^2 \simeq 10\text{--}20$ .

It is important to note that Eq. (3) has been obtained assuming that the cosmic ray number density  $n_{\text{cr}}$  is uniform, so that all the beam depolarization is attributed solely to the fluctuations in magnetic field. Under local equipartition,  $n_{\text{cr}} \propto B^2$ , Sokoloff et al. (1998, their Eq. (28)) calculated the degree of polarization at short wavelengths to be

$$p = p_0 \frac{1 + \frac{7}{3}\delta_b^2}{1 + 3\delta_b^2 + \frac{10}{9}\delta_b^4}.$$

As might be expected, this expression leads to a smaller  $\delta_b$  for a given  $p/p_0$  than Eq. (2):

$$\delta_b^2 \approx \frac{2p_0}{p} \quad \text{for } \frac{p}{p_0} \ll 1, \quad (4)$$

<sup>1</sup> It is useful to carefully distinguish between what can be called ‘pressure equality’ and ‘pressure equilibrium’: the former refers to the case where magnetic fields and cosmic rays have equal pressures locally, whereas the latter describes the situation where the sum of the two (or more) pressure contributions does not vary in space.

so that

$$\delta_b^2 \simeq 15 \quad \text{for } p = 0.1.$$

Since local equipartition between cosmic rays and magnetic fields maximizes beam depolarization, this is clearly a lower estimate of  $\delta_b$ .

The above estimates apply to statistically isotropic random magnetic fields. However, the random part of the interstellar magnetic field can be expected to be anisotropic at scales of order 100 pc, e.g., due to shearing by the galactic differential rotation, streaming motions and large-scale compression. Note that the anisotropy of MHD turbulence resulting from the nature of the spectral energy cascade (Lithwick et al. 2007; Galtier et al. 2000, and references therein) is important only at much smaller scales. Synchrotron emission arising in an anisotropic random magnetic field is polarized (Laing 1980; Sokoloff et al. 1998) and the resulting net polarization, from the combined random and mean field, can be either stronger or weaker than in the case of an isotropic random field depending on the sense of anisotropy relative to the orientation of the mean magnetic field.

The case of M33 provides a suitable illustration of the refinements required if the anisotropy of the random magnetic field is significant. Tabatabaei et al. (2008) obtained fractional polarization of about 0.1 at  $\lambda 3.6$  cm. Using Eq. (3), this yields  $\delta_b^2 \simeq 10$ , whereas Eq. (4) leads to  $\delta_b^2 \simeq 4$ , consistent with their equipartition estimates  $\sigma_b \simeq 6 \mu\text{G}$  and  $B_0 \simeq 2.5 \mu\text{G}$ . However, their analysis of Faraday rotation between  $\lambda 3.6$ , 6.2 and 20 cm suggests a weaker regular magnetic field,  $B_0 \simeq 1 \mu\text{G}$ , leading to  $\delta_b^2 \simeq 40$  if  $\sigma_b \simeq 6 \mu\text{G}$ .

The latter estimate for  $B_0$  is more reliable since using the degree of polarization can lead to an underestimated  $\delta_b$  because of anisotropy of the random magnetic field. Sokoloff et al. (1998, their Eq. (19)) have shown that the degree of polarization at short wavelengths in a partially ordered, anisotropic magnetic field is given by

$$p = p_0 \frac{1 + \delta_{by}^2(1 - \alpha_b^2)}{1 + \delta_{by}^2(1 + \alpha_b^2)},$$

where we have assumed, for the sake of simplicity, that  $B_y = B_0$  and  $B_x = 0$ , defined  $\delta_{by}^2 = \sigma_{by}^2/B_0^2$  and likewise for  $\delta_{bx}$ , and introduced  $\alpha_b^2 = \sigma_{bx}^2/\sigma_{by}^2$  ( $< 1$ ) as a measure of the anisotropy of  $\mathbf{b}_\perp$ . This approximation is relevant to spiral galaxies where the mean magnetic field is predominantly azimuthal (nearly aligned with the  $y$ -axis of the local reference frame used here) and the anisotropy in the random magnetic field is produced by the rotational shear,  $\sigma_{by} > \sigma_{bx}$ . For  $\delta_{by}^2 \gg 1$ , this yields, for  $p = 0.1$ ,

$$\alpha_b^2 \approx \frac{p_0 - p}{p_0 + p} \approx 0.8.$$

Thus, a rather weak anisotropy of the random magnetic field can produce  $p \sim 0.1$  and this allows us to reconcile the different estimates of  $\delta_b$  obtained from the degree of polarization and Faraday rotation in M33. The required anisotropy can be readily produced by the galactic differential rotation. Shearing of an initially isotropic random magnetic field leads, within one eddy turnover time, to an increase of its azimuthal component of

$$\sigma_{by} \simeq \sigma_{bx} \left( 1 - r \frac{d\Omega}{dr} \frac{l}{v} \right),$$

where  $\Omega(r)$  is the angular velocity of the galactic rotation (with the rotational velocity along the local  $y$ -direction and  $r$  the galactocen-

tric radius),  $l$  and  $v$  are the correlation length<sup>2</sup> and r.m.s. speed of the interstellar turbulence, so that  $l/v$  is the lifetime of a turbulent eddy. This leads to

$$\alpha_b \simeq \left( 1 - r \frac{d\Omega}{dr} \frac{l}{v} \right)^{-1} \simeq 1 - \frac{lV_0}{R_0v},$$

where the last equality is based on the estimate  $r d\Omega/dr \simeq -V_0/R_0$ , with  $V_0 = 107 \text{ km s}^{-1}$  and  $R_0 = 8 \text{ kpc}$  being the parameters of Brandt's approximation to the rotation curve of M33 (Rogstad et al. 1976). With  $l = 0.1 \text{ kpc}$  and  $v = 10 \text{ km s}^{-1}$ , we obtain  $\alpha_b^2 \simeq 0.8$ , in a perfect agreement with the degree of anisotropy required to explain the observations of Tabatabaei et al. (2008).

To conclude, a typical value of the relative strength of the random magnetic field in spiral galaxies is, at least,

$$\delta_b^2 \simeq 10. \quad (5)$$

This estimate refers to the correlation scale of interstellar turbulence,  $l \simeq 50\text{--}100 \text{ pc}$ . Higher values,  $\delta_b^2 \simeq 40$  are perhaps more plausible, but our results are not very sensitive to this difference (see Fig. 1 and Section 3).

### 3 SYNCHROTRON INTENSITY FLUCTUATIONS

The ratio of the fluctuating-to-mean synchrotron intensity in the interstellar medium (ISM) is sensitive to the relative distributions of cosmic ray electrons and magnetic fields and hence to the extent that energy equipartition may hold locally: the synchrotron emission will fluctuate strongly if equipartition holds pointwise, i.e., if the number density of cosmic ray electrons is increased where the local magnetic field is stronger. (We assume that cosmic ray electrons and heavier particles are similarly distributed – see Section 8 for the justification.) We estimate the area-averaged synchrotron intensity  $I_0 = \langle I \rangle_S$  in the plane of the sky and the standard deviation of the intensity fluctuations,  $\sigma_I = \sqrt{\langle I^2 \rangle_S - \langle I \rangle_S^2}$ , from the statistically homogeneous, diffuse ISM. Assuming for simplicity that the synchrotron spectral index is equal to  $-1$ , the total intensity of synchrotron emission is given by

$$I = \int_L \varepsilon ds \propto \int_L n_{\text{cr}} B_\perp^2 ds, \quad (6)$$

where  $\varepsilon$  is the synchrotron emissivity,  $n_{\text{cr}}$  is the number density of cosmic ray electrons,  $B_\perp$  is magnetic field in the plane of the sky and integration is carried along the line of sight  $s$  over the path-length  $L$ .

The relative fluctuations in the synchrotron intensity in the case of detailed (local, or pointwise) equipartition between cosmic rays and magnetic fields,  $n_{\text{cr}} \propto B^2$  can be estimated as (see Appendix A)

$$\delta_I \equiv \frac{\sigma_I}{I_0} = \frac{\delta_b(54 + 295\delta_b^2 + 404\delta_b^4 + 101\delta_b^6)^{1/2}}{N^{1/2}(3 + 10\delta_b^2 + 5\delta_b^4)}, \quad (7)$$

where  $N$  is the number of correlation cells of the synchrotron fluctuations within the telescope beam, and each vector component of

<sup>2</sup> The correlation length is also known as the integral scale and is defined as the integral of the variance-normalized autocorrelation function of a random variable. The typical linear size, or diameter, of a turbulent cell is  $2l$ .

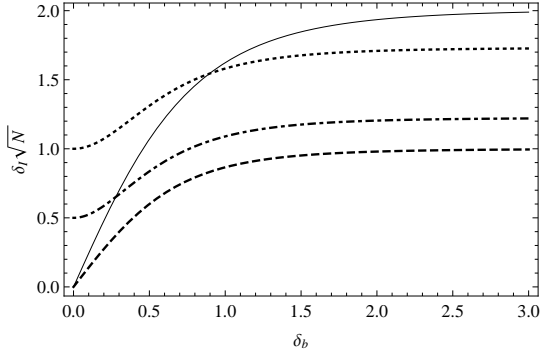


**Figure 1.** The relative fluctuations in synchrotron intensity  $\delta_I$  for special cases: complete correlation of cosmic rays and magnetic fields (solid),  $n_{cr} = \text{const}$  with fluctuating  $b$  (dashed) and uncorrelated fluctuations in cosmic rays and magnetic field, with  $\delta_n = 1$  (dotted) and  $\delta_n = 0.5$  (dot-dashed). The corresponding analytical expressions can be obtained from the formulae presented in Appendix A and Section 3. We note that the curves rapidly approach the horizontal asymptote, and the approximation  $\delta_b \rightarrow \infty$  is reasonably accurate for  $\delta_b > 1.5$ –2.

the magnetic field is assumed to be an independent Gaussian random variable of the same variance (i.e. an isotropic random magnetic field), and we recall that  $\delta_b = \sigma_b/B_0$ . As  $\delta_b$  increases,  $\delta_I$  rapidly approaches the asymptotic value

$$\delta_I \approx 2N^{-1/2} \quad \text{for } \delta_b^2 \gg 1.$$

It is useful to note similar expressions for  $\delta_I$  obtained under different assumptions about the correlation between cosmic rays and magnetic field. If cosmic ray fluctuations are statistically independent of those in magnetic field, with the mean value  $n_0 = \bar{n}_{cr}$  and standard deviation  $\sigma_n$ , we show in Appendix A that

$$\delta_I = \frac{[\delta_n^2 + \delta_b^2(2 + \delta_b^2)(1 + 2\delta_n^2)]^{1/2}}{N^{1/2}(1 + \delta_b^2)}, \quad (8)$$

where

$$\delta_n = \frac{\sigma_n}{n_0}$$

is the magnitude of the relative fluctuations in cosmic ray number density. In particular, for  $\delta_n \rightarrow 0$  we obtain an asymptotic form for a homogeneous distribution of cosmic rays:

$$\delta_I = \frac{\delta_b(2 + \delta_b^2)^{1/2}}{N^{1/2}(1 + \delta_b^2)}. \quad (9)$$

Thus,  $\delta_I \simeq N^{-1/2}$  for  $\delta_b^2 \gg 1$  and  $n_{cr} = \text{const}$ .

For the correlation length of the synchrotron fluctuations  $l_\epsilon = 50$  pc and the pathlength  $L = 1$  kpc, we obtain  $N = L/2l_\epsilon \simeq 10$  for a beam narrower than the size of the correlation cell. With Eq. (5), the relative magnitude of synchrotron fluctuations expected under detailed equipartition follows from Eq. (7) as

$$N^{1/2}\delta_I \approx 2.0 \quad (\text{local equipartition}). \quad (10)$$

Equation (8) yields, for  $\delta_n = 0.5$ ,

$$N^{1/2}\delta_I \approx 1.2 \quad (\text{uncorrelated fluctuations}),$$

and Eq. (9) leads to

$$N^{1/2}\delta_I \approx 1.0 \quad (n_{cr} = \text{const}).$$

As might be expected, detailed equipartition between cosmic rays and magnetic fields leads to the strongest synchrotron fluctuations for a given  $\delta_b$  and  $N$ . Figure 1 shows the dependencies defined by

Eqs (7), (8) and (9). We note that the dependence of  $\delta_I$  on  $\delta_b$  is quite weak as long as  $\delta_b^2 \gtrsim 3$ .

## 4 SYNCHROTRON FLUCTUATIONS IN THE MILKY WAY AND M33

In this section we estimate the relative level of synchrotron fluctuations from observations of the Milky Way and the spiral galaxy M33. An ideal data set for this analysis should (i) resolve the fluctuations at their largest scale, (ii) only include emission from the ISM and not from discrete sources such as AGN and stars, (iii) not be dominated by structures that are large and bright due to their proximity, such as the North Polar Spur, (iv) be free of systematic trends such as arm-interarm variations or vertical stratification. The data should allow the ratio  $\delta_I = \sigma_I/I_0$  to be calculated separately in arm and inter-arm regions or at low and high latitudes as  $I_0$  differs between these regions. Regarding item (i) above, we note that a turbulent cell of 100 pc in size subtends the angle of about  $6^\circ$  at a distance of 1 kpc. Furthermore, most useful for our purposes are long wavelengths where the contribution of thermal radio emission is minimum. Unfortunately, ideal data satisfying all these criteria do not exist; we therefore use several radio maps, where each map possesses a few of the desirable properties listed above and collectively they have them all.

### 4.1 The data

#### 4.1.1 The 408 MHz all-sky survey

The survey of Haslam et al. (1982) covers the entire sky at a resolution of  $51'$  and with an estimated noise level of about 0.67 K. Synchrotron radiation is the dominant contribution to emission at the survey's wavelength of  $\lambda 74$  cm. The brightest structures in the map shown in Fig. 2a are the Galactic plane and several arcs due to nearby objects, especially the North Polar Spur.

#### 4.1.2 The 408 MHz all-sky survey, without discrete sources

La Porta et al. (2008) removed the strongest discrete sources from the data of Haslam et al. (1982) using a two-dimensional Gaussian filter. We compared the results obtained from the original 408 MHz survey with those from this map to show that the effect of point sources on our results is negligible.

#### 4.1.3 The 22 MHz part-sky survey

Roger et al. (1999) produced a map, shown in Fig. 3a, of about 73% of the sky at  $\lambda 13.6$  m, between declinations  $-28^\circ$  and  $+80^\circ$  at a resolution of approximately  $1^\circ \times 2^\circ$  and an estimated noise level of 5 kK. The emission is all synchrotron radiation, but H II regions in the Galactic plane absorb some background emission at this low frequency. However, we are most interested in regions away from the Galactic plane, so our conclusions are not affected by the absorption in the H II regions. The brightest point sources were removed by Roger et al. (1999) as they produced strong side-lobe contamination in the maps: this accounts for the four empty rectangles in Fig. 3a.

We expect that results useful for our purposes arise at the angular scale of about  $6^\circ$  in all three Milky Way maps (i.e., the angular size of a turbulent cell at a 1 kpc distance), whereas larger scales isolate regular spatial variations of the radio intensity.

#### 4.1.4 The 1.4 GHz map of M33

The nearby, moderately inclined, spiral galaxy M33 was observed at  $\lambda 21$  cm by Tabatabaei et al. (2007a), using the VLA and Effelsberg 100 m telescopes, at a resolution of  $51''$ , or about 200 pc at the distance to M33 of 840 kpc. The noise level is estimated to be 0.07 mJy/beam. The resolution is sufficient to resolve arm and inter-arm regions, but is at the top end of the expected scale of random fluctuations due to turbulence. The beam area includes a few (nominally, four) correlation cells of the synchrotron fluctuations. The emission is a mixture of thermal and synchrotron radiation. The overall thermal fraction is estimated to be 18% but it is strongly enhanced in large H II regions and spiral arms (Tabatabaei et al. 2007b) whereas the synchrotron emission comes from the whole disc. The radio map used here is shown in Fig. 4a. The spiral pattern is notably weak in total synchrotron intensity, so the map appears almost featureless. This makes this galaxy especially well suited for our analysis since we are interested in quasi-homogeneous random fluctuations of the radio intensity. Nevertheless, systematic trends are noticeable in this map and we discuss their removal in Section 4.2.3.

#### 4.2 Statistical parameters of the synchrotron fluctuations

For the three Milky Way data sets of Sections 4.1.1–4.1.3, we calculated the mean  $I_0$  and standard deviation  $\sigma_I$  of the synchrotron intensity  $I$  at each point in the map. In each case, the data were smoothed with a Gaussian of an angular width  $a$ , resulting in the local mean intensity at the scale  $a$ , which we denote  $I_{0a}$ :

$$I_{0a} = S_a^{-1} \iint I(l', b') \exp(-\theta^2/a^2) \cos b \, dl' \, db', \quad (11)$$

where integration extends over the data area,  $\mathbf{r} = (l, b)$  is the position vector on the unit sky sphere, with  $l$  and  $b$  the Galactic longitude and latitude (confusion with the small-scale magnetic field, denoted here  $\mathbf{b}$ , should be avoided),  $\theta = \arccos(\mathbf{r} \cdot \mathbf{r}')$  is the angular separation between  $\mathbf{r}$  and  $\mathbf{r}'$ ,

$$S_a(l, b) = \iint \exp(-\theta^2/a^2) \cos b \, dl' \, db',$$

is the averaging area, and the integration extends over the whole area of the sky available in a given survey. The standard deviation  $\sigma_{Ia}$  of radio intensity at a given position  $(l, b)$  at a given scale  $a$  is calculated as

$$\sigma_{Ia}^2(l, b) = \langle I^2 \rangle_a - \langle I \rangle_a^2,$$

where angular brackets denote averaging defined as in Eq. (11).

In the case of M33, we selected nine areas which avoid the brightest H II regions and whose radio continuum emission is thus likely to be dominated by synchrotron radiation. Each area encompasses several beams and  $\delta_I$  was calculated in each, using the mean value and the standard deviation of  $I$  among all the pixels in the field obtained after removing regular trends.

#### 4.2.1 The 408 MHz survey

To reduce the influence of the Galactic disc, where the complicated structure in the radio maps is mainly due to systematic arm-interarm variations and localized radio sources such as supernova remnants, the original intensity data were truncated at 52 K (1% of the maximum and 167% of the r.m.s. value of  $I$ ). The resulting sky distribution of the relative radio intensity fluctuations  $\sigma_{Ia}/I_{0a}$  is

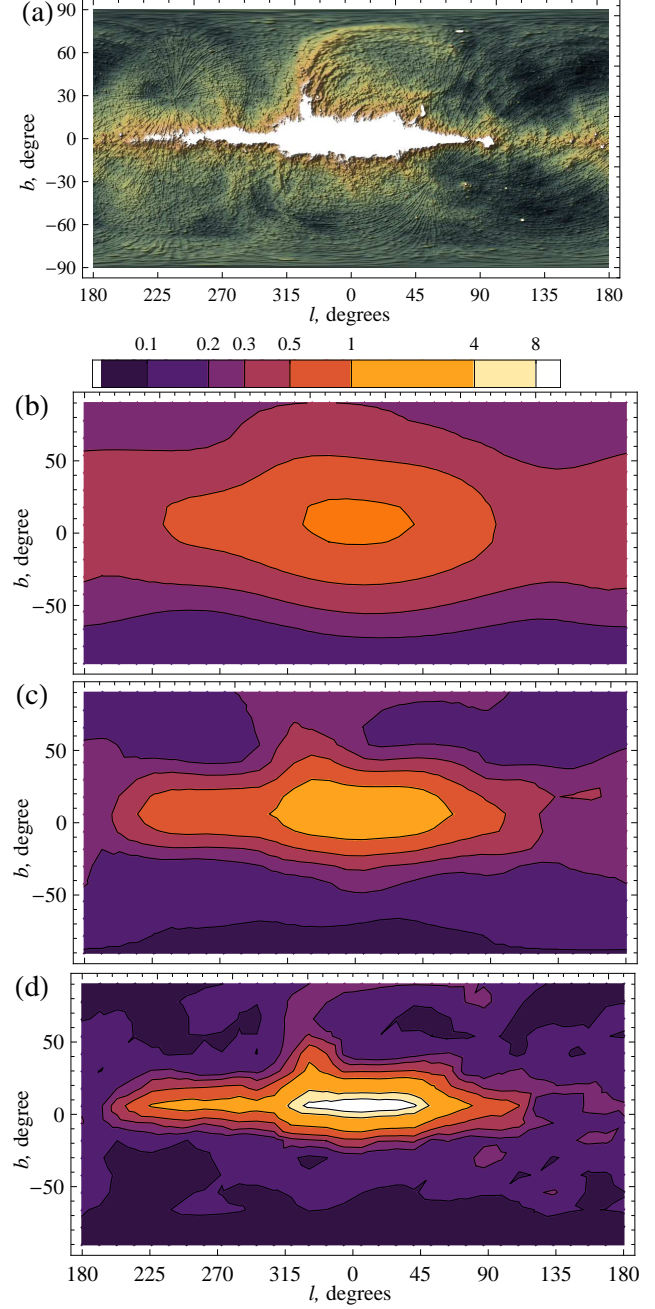


**Figure 2.** (a): The 408 MHz all-sky map of the total synchrotron intensity (Haslam et al. 1982), with the Galactic disc area ( $I > 52$  K) blanked out. The lower panels show the magnitude of the relative fluctuations of the synchrotron intensity,  $\delta_I = \sigma_I/I_0$ , at various scales: (b)  $a = 30^\circ$ , (c)  $a = 15^\circ$  and (d)  $a = 7^\circ$ . The latter scale is about the angular size of a turbulent cell ( $2l_\varepsilon = 100$  pc) seen at a distance 1 kpc.

shown in Fig. 2 for a selection of averaging scales,  $a = 30^\circ$ ,  $15^\circ$  and  $7^\circ$  ( $a$  corresponds to the radius rather than the diameter of the region).

While panels (b) and (c) in Fig. 2 reflect mainly systematic trends in radio intensity, we expect that panel (d) is dominated by the turbulent fluctuations. In particular, the  $a = 7^\circ$  map shows a much weaker variation with Galactic latitude than those at larger scales, for  $|b| \gtrsim 20^\circ$ . We note that the correlation scale of the syn-

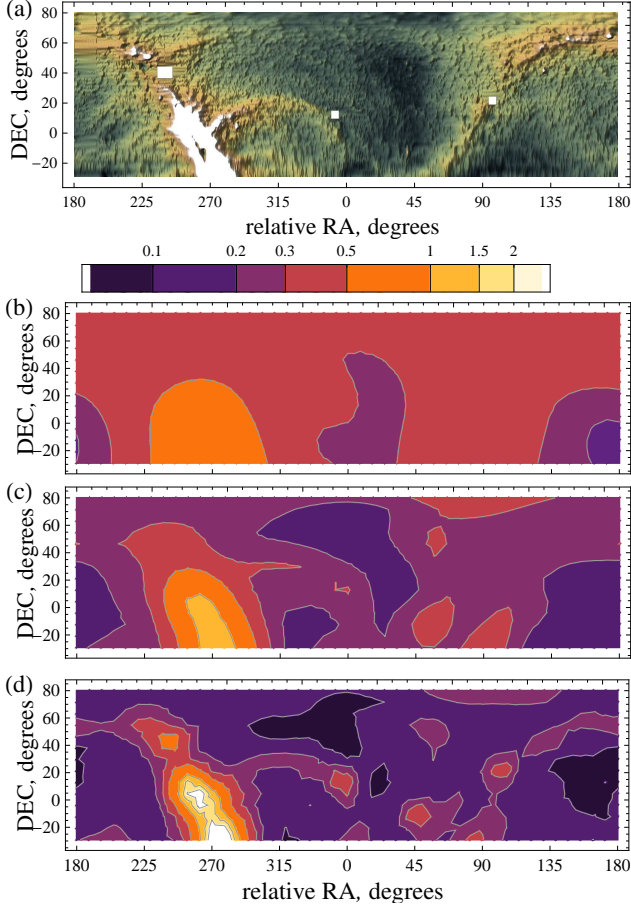


**Figure 3.** As in Fig. 2 but for the 22 MHz survey (Roger et al. 1999).

chrotron fluctuations obtained by Dagkesamanskii & Shutenkov (1987) is  $8^\circ$ .

Contours outside the Galactic disc in Fig. 2d,  $|b| \gtrsim 20^\circ$  give

$$\frac{\sigma_I}{I_0} = 0.1\text{--}0.2. \quad (12)$$

Results obtained from the 408 MHz map with point sources subtracted differ insignificantly from those obtained using the original map.

#### 4.2.2 The 22 MHz partial sky survey

Contours of the relative intensity fluctuations obtained from the 22 MHz map are shown in Fig. 3. As in Fig. 2, averaging over scales  $a = 30^\circ$  and  $15^\circ$  reveals the large-scale structure clearly visible in the original data. However, results at  $a = 7^\circ$  show much less of such structure, and the statistically homogeneous part of the sky in this panel includes the same contours of 0.1 and 0.2 as in Fig. 2, with the value of 0.3 confined to the bright ridges seen in Fig. 3a. Thus, the 22 MHz data are in a good agreement with the values for  $\delta_I$  obtained from the 408 MHz data. This suggests a weak frequency dependence of the relative synchrotron fluctuations  $\delta_I$ .

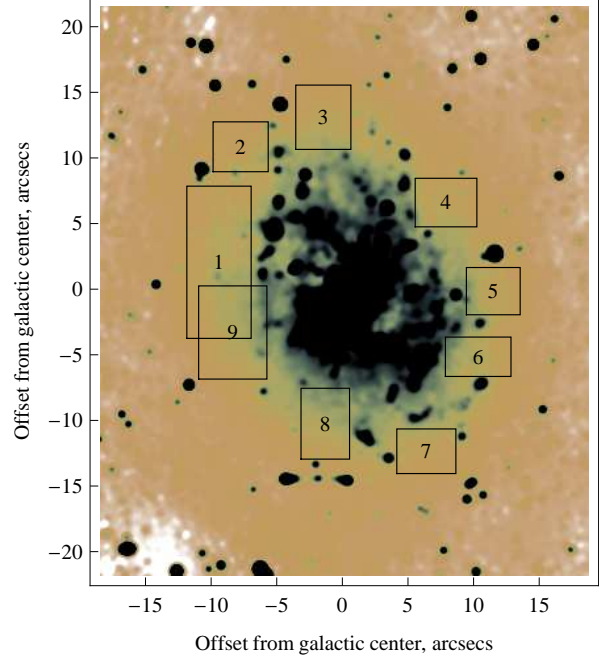


**Figure 4.** The 1.4 GHz radio map of M33 (Tabatabaei et al. 2007a), with the rectangular fields used in our analysis shown. For orientation, we note that the size of Field 3 is  $7' \times 7'$  equivalent to  $1.6 \times 1.9 \text{ kpc}^2$ .

**Table 1.** Relative radio intensity fluctuations  $\sigma_I/I_0$  in M33 with systematic trends of various orders subtracted. The first column gives the field number as specified in Fig. 4, and the next three columns show the relative fluctuations of radio intensity, with  $\sigma_I^{(m)}$  the standard deviation of  $I$  within a given field, obtained with a trend of order  $m$  and zero mean value subtracted:  $m = 0$  corresponds to the original data,  $m = 1$ , to a linear trend, and  $m = 2$ , to a quadratic trend in the angular coordinates. The last column shows the mean value of the radio intensity in each field.

Field No.	$\sigma_I^{(0)}/I_0$	$\sigma_I^{(1)}/I_0$	$\sigma_I^{(2)}/I_0$	$I_0 [\mu\text{Jy/beam}]$
1	0.30	0.18	0.14	677
2	0.34	0.22	0.19	545
3	0.31	0.15	0.11	609
4	0.28	0.18	0.17	606
5	0.38	0.17	0.13	672
6	0.35	0.15	0.12	795
7	0.30	0.16	0.14	565
8	0.32	0.07	0.07	902
9	0.38	0.14	0.11	810
Mean	0.33	0.16	0.13	687

#### 4.2.3 M33

Our analysis for the Milky Way has a potential difficulty that long lines of sight might make it impossible to separate the contributions to  $\sigma_I$  from small-scale (random) and large-scale (systematic) variations of the synchrotron emissivity. Therefore, we consider also the nearby galaxy M33 seen nearly face-on (inclination  $56^\circ$ ). To avoid excessive contribution from large-scale variations due to the spiral pattern and the radial gradient in  $I$ , we selected relatively small fields shown in Fig. 4, selecting areas free of strong star formation in the outer regions of the galaxy disc. The areas of the rectangular fields chosen range from  $1.9 \times 1.2 \text{ kpc}^2$  to  $1.9 \times 4.7 \text{ kpc}^2$ .



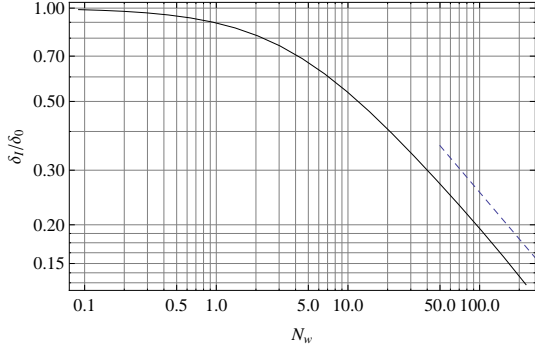


**Figure 5.** The relative fluctuations in synchrotron intensity  $\delta_I$  as a function of  $N_W$ , the number of synchrotron correlation cells across the beam area, with  $\delta_I$  normalized by  $\delta_0$ , the relative fluctuations obtained along a single line of sight, i.e., for  $N_W = 0$ . The asymptotic dependence  $\delta_I = 2\delta_0 N_W^{-1/2}$  emerges only for  $N_W \gtrsim 20$ –30. The calculation assumed a Gaussian beam, with the full width at half-maximum (FWHM) taken for the beam diameter.

The fields are big enough to make gradients in the mean quantities significant; in particular, the non-thermal disc of M33 has a strong radial gradient in radio intensity (Tabatabaei et al. 2007b), so we subtract regular trends from the values of  $I$ . We fitted first- or second-order polynomials to  $I(l, b)$  in  $l$  and  $b$  in each field and calculated  $\delta_I$  after subtracting the trends with zero mean value from the original data. Results are shown in Table 1, with  $\sigma_I^{(m)}$  denoting the standard deviation of the radio intensity obtained upon the subtraction of a polynomial of order  $m$  in the angular coordinates. The mean value of synchrotron intensity  $I_0$  was calculated for each field.

We note that  $\sigma_I^{(0)}$  (the standard deviation of  $I$  in the original data) is noticeably larger than  $\sigma_I^{(1)}$  and  $\sigma_I^{(2)}$ . Thus, the large-scale trends contribute significantly to the intensity variations. On the other hand,  $\sigma_I^{(1)}$  and  $\sigma_I^{(2)}$  have rather similar magnitudes of order 0.15 (and  $\sigma_I^{(1)} > \sigma_I^{(2)}$  as expected), so that they can be adopted as an estimate of  $\sigma_I$  corrected for the large-scale trends. We use the value of  $\sigma_I^{(2)}/I_0$  averaged over the nine fields explored as the best estimate for  $\delta_I$ .

However,  $W \approx 100$  pc (half-width at half maximum of the Gaussian beam) in the observations of M33 used here, and the beam area encompasses  $N_W \approx 4$  correlation cells. For comparison with the Milky Way data, this estimate has to be reduced to the virtually perfect resolution available in the Milky Way. For such a small value of  $N_W$  as in the high-resolution observations of M33, the dependence of  $\delta_I$  differs significantly from its asymptotic form  $\delta_I \propto N_W^{-1/2}$ . Figure 5 shows the dependence of  $\delta_I$  on  $N_W$  obtained for a model synchrotron-emitting system described in detail in Section 5:  $\delta_I$  only weakly depends on  $N_W$  for small  $N_W$ . Reduced to a single line of sight, the synchrotron fluctuations in M33 then correspond to  $\delta_I = 0.2$  if the synchrotron correlation length is  $l_\varepsilon = 50$  pc (i.e.,  $N_W = 4$ ). We also recall that the typical path-length through M33 is twice that through the Milky Way, and we adopt  $L = 2$  kpc for this galaxy. Then the value of  $\delta_I$  in M33, reduced to  $L = 1$  kpc for compatibility with the Milky Way data, is further  $\sqrt{2}$  times larger:

$$\delta_I \simeq 0.3.$$

### 4.3 Comparison with earlier results and summary

Synchrotron observations in the Milky Way focus primarily on the spectrum of the fluctuations while their magnitude has attracted surprisingly little attention. Mills & Slee (1957) observed fluctuations of the Galactic radio background near the Galactic south pole at  $\lambda = 3.5$  m, with the resolution of  $50^\circ$ , to obtain  $\sigma_I = 3.3 \times 10^{-26} \text{ W m}^{-2} \text{ Hz}^{-1}$  per beam, which corresponds to  $\delta_I = 0.12$  (see also Getmantsev 1959).

Dagkesamanskii & Shutenkov (1987) used observations at 102.5 MHz ( $\lambda 2.92$  m) near the North Galactic Pole, where the Galactic radio emission is minimum, to determine the synchrotron autocorrelation function and its anisotropy arising from the large-scale magnetic field. They obtain  $\delta_I \approx 0.07$  but note that this estimate should be doubled if the isotropic extragalactic background (half the total flux) is to be subtracted, to yield  $\delta_I \simeq 0.14$ . Banday et al. (1991a) argue that only 17% of the total flux is of extragalactic origin, and then  $\delta_I \simeq 0.08$  at 102.5 MHz.

The autocorrelation function of the brightness temperature fluctuations of the Galactic radio background was determined also by Banday et al. (1991a,b) who used observations at 408 and 1420 MHz, smoothed to a resolution of about FWHM =  $5^\circ$ . They observed a ‘quiet’ region with reduced fluctuations,  $30^\circ < \text{DEC} < 50^\circ$ ,  $180^\circ < \text{RA} < 250^\circ$ , identified by Bridle (1967) as an inter-arm region, since they were interested in the cosmic microwave background fluctuations. For the Galactic synchrotron radiation, which dominates at these frequencies, they obtain  $\delta_I \approx 0.05$  at 408 MHz and 0.08 at 1420 MHz.

These estimates are somewhat lower than those obtained in Section 4. The value of  $\delta_I$  obtained by Banday et al. can be lower due to their selection of a region with weaker synchrotron fluctuations.

The relative fluctuations in radio intensity are remarkably similar in all the Milky Way maps and in all fields in M33 considered, with

$$\delta_I \equiv \sigma_I/I_0 \approx 0.1\text{--}0.3,$$

when reduced to the common pathlength  $L = 1$  kpc (see Section 6.2 for further discussion). The lower values are more plausible. We believe that these estimates are not significantly affected by either large-scale trends in the radio intensity or by discrete radio sources or by thermal emission. Even if these effects still contribute to our estimate, it provides an *upper* estimate of the fluctuations in synchrotron intensity arising in the interstellar medium of the Milky Way and M33.

## 5 MAGNETIC FIELD AND COSMIC RAY MODEL

In order to interpret the results of our analysis of observations in Section 4, we use a model of a partially ordered random magnetic fields and an associated distribution of cosmic rays, assuming various degrees of correlation (or anticorrelation) between these two components. We then calculate the synchrotron intensity from a computational box of appropriate size and compare the result with the observational constraints described above in order to establish the degree of correlation or anticorrelation compatible with observations.

The model magnetic field is described as a sum of a mean and random component,  $\mathbf{B}_0$  and  $\mathbf{b}$ , respectively:

$$\mathbf{B} = \mathbf{B}_0 + \mathbf{b},$$

with volume averages  $\langle \mathbf{b} \rangle = 0$ ,  $\langle \mathbf{B} \rangle = \mathbf{B}_0$  and  $\langle B^2 \rangle = B_0^2 +$

$B_{0\parallel}^2 + \sigma_b^2$ , where  $B_{0\perp}$  and  $B_{0\parallel}$  are the mean field components in the plane of the sky and parallel to the line of sight, respectively.

### 5.1 A model of a partially ordered magnetic field

To prescribe a quasi-random magnetic field  $\mathbf{b}$  with vanishing mean value in a periodic box, we use a Fourier expansion in modes with randomly chosen directions of wave vectors  $\mathbf{k}$ , but with amplitudes adjusted to reproduce any desired energy spectrum:

$$\mathbf{b}(\mathbf{x}) = \frac{1}{(2\pi)^{3/2}} \int \hat{\mathbf{b}}(\mathbf{k}) e^{i\mathbf{k}\cdot\mathbf{x}} d^3\mathbf{k}, \quad (13)$$

where  $\hat{\mathbf{b}}$  is the Fourier transform of  $\mathbf{b}$ ; the physical field is represented by the real part of this complex vector. The corresponding magnetic energy spectrum is given by

$$M(k) = \int_{|\mathbf{k}'|=k} |\hat{\mathbf{b}}(\mathbf{k}')|^2 d^3\mathbf{k}', \quad (14)$$

where the integral is taken over the spherical surface of a radius  $k$  in the  $k$ -space. In the isotropic case,  $M(k) = 4\pi k^2 |\hat{\mathbf{b}}(k)|^2$ . In order to ensure periodicity within a computational box of size  $L$ , as required for the discrete Fourier transformation, the components of the wave vectors are restricted to be integer multiples of  $2\pi/L$ .

A solenoidal vector field  $\mathbf{b}$ , i.e., that having  $\nabla \cdot \mathbf{b} = \mathbf{k} \cdot \hat{\mathbf{b}}(\mathbf{k}) = 0$ , is then obtained from  $\mathbf{k}$  and  $M(k)$  as

$$\hat{\mathbf{b}}(\mathbf{k}) = \frac{\mathbf{k} \times \mathbf{X}}{|\mathbf{k} \times \mathbf{X}|} k^{-1} \sqrt{M(k)},$$

where  $\mathbf{X}$  is a complex vector chosen at random, to ensure that the Fourier modes have random phases. We consider a magnetic energy spectrum represented by two power-law ranges,

$$M(k) = M_0 \begin{cases} (k/k_0)^{s_0} & \text{for } k < k_0, \\ (k/k_0)^{-s_1} & \text{for } k \geq k_0, \end{cases}$$

with  $s_0 > 0$  and  $s_1 > 0$ , where  $k_0$  is the energy-range wavenumber. We use  $s_1 = 5/3$  as in Kolmogorov's spectrum and  $s_0 = 2$  (see Christensson et al. 2001). The standard deviation of the magnetic field is given by

$$\sigma_b^2 = \int_0^\infty M(k) dk = M_0 k_0 \frac{s_0 + s_1}{(s_0 + 1)(s_1 - 1)}$$

for  $s_1 > 1$ . The correlation length  $l_b$  of the resulting magnetic field (analogous to the radius of a correlation cell) differs from its dominant half-wavelength  $\frac{1}{2}\lambda_0 = \pi/k_0$  for any finite values of  $s_0$  and  $s_1$ :

$$\begin{aligned} l_b &= \frac{\pi}{2} \frac{\int_0^\infty k^{-1} M(k) dk}{\int_0^\infty M(k) dk} = \frac{\pi}{2k_0} \left(1 + \frac{1}{s_0}\right) \left(1 - \frac{1}{s_1}\right) \\ &= \frac{3\pi}{10k_0}, \end{aligned} \quad (15)$$

where the last equality follows for  $s_0 = 2$  and  $s_1 = 5/3$ .

The resulting solenoidal vector field is then added to a uniform component  $\mathbf{B}_0$  to produce a partially ordered magnetic field with controlled fluctuation level  $\delta_b$  and energy spectrum  $M(k)$ . This approach has been used to generate synthetic polarization maps of the turbulent ISM by Stepanov et al. (2008); Volegova & Stepanov (2010); Arshakian et al. (2011); Moss et al. (2012). Similar constructions were used by Giacalone & Jokipii (1999) and Casse et al. (2002) in their modelling of cosmic ray propagation in random magnetic fields, by Malik & Vassilicos (1999) for modelling turbulent flows, and by Wilkin et al. (2007) to study dynamo action in chaotic flows.

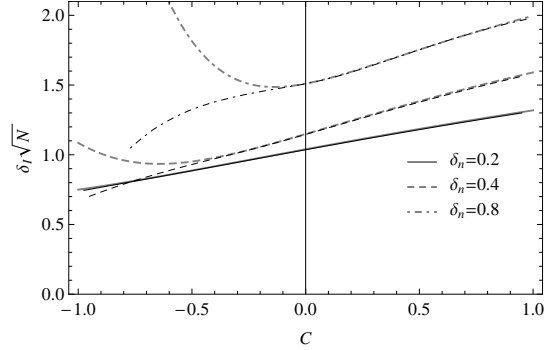


**Figure 6.** The relative fluctuations in synchrotron intensity  $\delta_I$  as obtained from analytical formulae Eqs. (A3 and (A4)) (thicker curves) and from numerical calculations with the condition  $n_{\text{cr}} > 0$  enforced (the corresponding thinner curves), for:  $\delta_n = 0.2$  (solid),  $\delta_n = 0.4$  (dashed) and  $\delta_n = 0.8$  (dash-dotted). The analytic formulae become inapplicable for  $C < 0$  and  $\delta_n \simeq 1$  (see the text). The magnetic field is purely random,  $B_0 = 0$  and  $N = 10$ .

### 5.2 Cosmic ray distribution partially correlated with magnetic field

Now we introduce a random distribution of cosmic rays which has a prescribed cross-correlation coefficient with the total magnetic energy density  $B^2/8\pi$  for the magnetic field described in Section 5.1. We first generate another, independent realization of the magnetic field,  $\mathbf{B}'$  using the same procedure as above, but with different randomly selected vectors  $\mathbf{X}$  and  $\mathbf{B}'_0 = 0$ . By construction,  $B^2$  and  $B'^2$  are uncorrelated scalar fields,

$$C(B^2, B'^2) = 0, \quad (16)$$

where

$$C(u, v) = \frac{\langle uv \rangle - \langle u \rangle \langle v \rangle}{\sigma_u \sigma_v},$$

is the cross-correlation coefficient of the random variables  $u$  and  $v$ , with  $C = 1$  if  $u$  and  $v$  are perfectly correlated and  $C = -1$  for perfectly anticorrelated  $u$  and  $v$ . The number density of cosmic rays is then obtained as

$$n_{\text{cr}} = \delta_n \left[ \alpha (B^2 - \langle B^2 \rangle) + \beta (B'^2 - \langle B'^2 \rangle) \right] + 1, \quad (17)$$

where  $\alpha = C/\sigma_{B^2}$  and  $\beta = \sqrt{1 - C^2}/\sigma_{B'^2}$  (see Appendix A for details). Here

$$\sigma_{B^2} = \left[ \frac{2}{3} \sigma_b^2 (2B_0^2 + \sigma_b^2) \right]^{1/2}$$

is the standard deviation of  $B^2$ , and  $\sigma_{B'^2}$  is that of  $B'^2$ . Equation (17) ensures that

$$\langle n \rangle_{\text{cr}} \equiv n_0 = 1, \quad \sigma_n = \delta_n;$$

in other words, the number density of cosmic rays  $n_{\text{cr}}$  is measured in the units of  $n_0$ .

This model is flexible enough to admit control over the spectrum of cosmic-ray density fluctuations by a suitable choice of the spectrum of  $\mathbf{B}'$ . However, we do not use this opportunity, and  $\mathbf{B}$  and  $\mathbf{B}'$  always have identical spectra.

We will now verify, by direct calculation, that  $C(B^2, n_{\text{cr}}) \approx C$ . The reason for the approximate equality is first explained.

A shortcoming of this cosmic-ray model is that  $n_{\text{cr}}$  can be negative at some positions (especially when  $C < 0$  and hence  $\alpha < 0$ ) because, at some positions and in some realizations,  $B^2$  can



be arbitrarily large (as a Gaussian random variable squared). This deficiency could be corrected by selecting a more realistic probability distribution for  $\mathbf{b}$  (e.g., a truncated Gaussian) but we do not feel that this would lead to any additional insight. In the numerical calculations described below, we truncate the negative values of  $n_{\text{cr}}$  replacing them by zero. This, however, makes it impossible to achieve exact anticorrelation between cosmic rays and magnetic fields, so that  $C(B^2, n_{\text{cr}}) > -1$ . As shown in Fig. 6, this constraint is not restrictive for  $\delta_n \lesssim 1$ , where  $C = -1$  is achievable with high accuracy; however, for  $\delta_n = 0.8$  the typical smallest value of  $C$  is about  $-0.8$ . Enforcing  $n_{\text{cr}} = 0$  at positions where  $B^2$  is exceptionally large can lead to a reduction in the values of  $\sigma_I$  obtained.

In analytical calculations, we restrict ourselves to the cases with  $\delta_n < 1$  to reduce the extent of the problem (even if not to resolve it completely). For example, Eqs. (A3) and (A4) yield for  $B_0 \rightarrow 0$  (i.e.,  $\delta_b \rightarrow \infty$ )

$$\delta_I = \frac{[9 + 6\delta_n (11C^2\delta_n + 3\sqrt{6}C + 3\delta_n)]^{1/2}}{N^{1/2}(\sqrt{6}C\delta_n + 3)}. \quad (18)$$

This dependence of  $\delta_I$  on the cross-correlation coefficient  $C$  is shown with thicker curves in Fig. 6 for various values of the relative fluctuations in cosmic rays,  $\delta_n$ . Thinner curves show similar results obtained from a numerical calculation where  $n_{\text{cr}} > 0$  is enforced. It is clear from Fig. 6 that these analytical results are accurate for  $C > 0$ . However, for  $C < 0$ , they are useful only if the fluctuations in the cosmic ray number density are relatively weak:  $C \gtrsim -0.1$  for  $\delta_n < 0.8$ ,  $C \gtrsim -0.5$  for  $\delta_n < 0.4$ , and almost any value of  $C$  for  $\delta_n < 0.2$ . We only use these analytical results for illustrative purposes, whereas all our conclusions are based on numerical results where  $n_{\text{cr}} > 0$  at all positions.

## 6 RESULTS

### 6.1 Synthetic radio maps

Each component of the magnetic field described by Eq. (13) is the sum of a large number of independent contributions from different wave numbers. By virtue of the central limit theorem, each component of the resulting magnetic field is well approximated by a Gaussian random variable. Then the mean synchrotron intensity and its standard deviation over  $N$  correlation cells can be expressed, using Eq. (6), in terms of  $B_0$ ,  $\sigma_b$ ,  $\delta_n$  and  $C$ . Explicit analytic expressions for  $I_0$  and  $\sigma_I$  can be found in Appendix A, and we illustrate these results in Fig. 6. As might be expected, the relative level of the synchrotron intensity fluctuations increases with the cross-correlation coefficient between  $B^2$  and  $n_{\text{cr}}$ .

Since analytical results are of limited relevance for  $C < 0$ , we performed numerical calculations of the synchrotron intensity where the cosmic-ray number density is truncated to be non-negative (i.e.  $n_{\text{cr}} = 0$  wherever the model defined by Eq. (17) returns a negative value). The model has four free parameters:

- (i) the relative level of magnetic field fluctuations  $\delta_b = \sigma_b/B_0$ ,
- (ii) the relative level of cosmic-ray number density fluctuations  $\delta_n = \sigma_n/n_0$ ,
- (iii) the cross-correlation coefficient between magnetic field and cosmic rays  $C$ , and
- (iv) the dominant energy wave number of the turbulent magnetic field  $k_0$ .

We do not vary the spectral index of magnetic field and cosmic rays as these parameters are of secondary importance in this context.

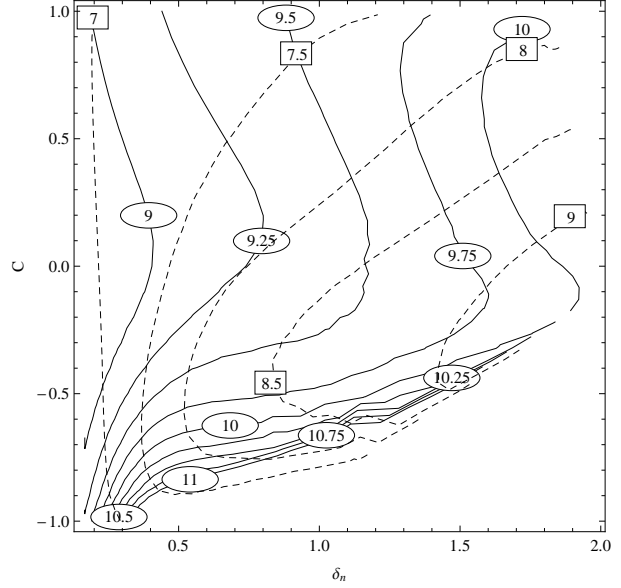


**Figure 7.** The isocontours of the numerical factor  $G$  in Eq. (20) for  $\sigma_b = 1$  (dashed lines and labels in squares) and  $\sigma_b \rightarrow \infty$  (solid lines and labels in ovals) shown in the  $(\delta_n, C)$ -plane.

The value of  $k_0$  controls the correlation lengths of magnetic field (Eq. (15)), cosmic rays and synchrotron emissivity, and hence the number of the correlation cells of synchrotron fluctuations in the telescope beam  $N$ , which in turn affects the magnitude of synchrotron fluctuation as  $\delta_I \propto N^{-1/2}$ . Since  $N$  can vary widely between different lines of sight in the Milky Way and between galaxies with different inclination angles, we present our results in terms of  $N^{1/2}\delta_I$  for both the observations and the model.

### 6.2 A relation between the correlation lengths of the synchrotron emissivity and magnetic field?

In the case of infinitely narrow beam, the number of synchrotron correlation cells traversed by the emission is just the ratio  $N = L/(2l_e)$ , where  $L$  is the pathlength through the synchrotron source and  $l_e$  is the correlation length of the fluctuations in the synchrotron emissivity. For a finite beam width  $W$ , this is the number of correlation cells within the beam cylinder,  $N \simeq (3/16)LW^2/l_e^3$ , assuming a circular beam and spherical correlation cells. Unlike the correlation lengths of physical parameters such as the magnetic field, velocity or density fluctuations, the correlation length of the intensity (or emissivity) variations cannot be deduced independently (e.g., from the nature of the turbulence driving), but has to be calculated from the statistical parameters of the physical variables or from observations.

To illustrate the difficulties arising, consider the autocorrelation function of  $b_\perp^2$  as an example. If  $V(x)$  is a stationary Gaussian random function, with vanishing mean value and the autocorrelation function  $K_v(r) = \overline{V(x)V(x+r)}$ , the autocorrelation function of  $W(x) = V^2(x)$  is given by  $K_w(r) = 2[K_v(r)]^2$  (see e.g. §13 in Sveshnikov 1966). Assuming that each component  $b_i$  of the random magnetic field is a Gaussian random variable, with the autocorrelation function  $K_{b_i}$ , we have  $K_{b_i^2} = 2K_{b_i}^2$ . Assuming statistical isotropy of  $\mathbf{b}$ ,  $K_{b_x}(r) = K_{b_y}(r)$ , and neglecting any cross-correlations between  $b_x$  and  $b_y$ , we obtain the autocorrelation

function of  $b_{\perp}^2$ :

$$K_{b_{\perp}^2}(r) = 4K_{b_i^2}(r).$$

Then relation between the correlation scales of  $b_i$  and  $b_{\perp}^2$ , denoted  $l_{b_i}$  and  $l_{b_{\perp}^2}$ , respectively, depends on the form of the autocorrelation function of magnetic field: for  $K_{b_i} = \frac{1}{3}\sigma_b^2 \exp(-r/l_b)$ , we have  $l_{b_{\perp}^2} = l_{b_i}/2$ . However, for  $K_{b_i} = \frac{1}{3}\sigma_b^2 \exp(-\pi r^2/l_b^2)$  we have  $l_{b_{\perp}^2} = l_{b_i}/\sqrt{2}$ . There is no universal relation between the correlation scales of even these simply connected variables. Such a relation should be established in each specific case from the statistical properties of each physical component of the system.

We calculate the correlation length  $l_{\varepsilon}$  of the synchrotron emissivity  $\varepsilon \propto n_{\text{cr}} B_{\perp}^2$  in the synthetic radio maps from its autocorrelation function  $K_{\varepsilon}(r)$ , for various values of the cross-correlation coefficients  $C$ ,  $B_0$  and  $n_0$ :

$$l_{\varepsilon} = \sigma_{\varepsilon}^{-2} \left( \int_0^L K_{\varepsilon}(r) dr - \langle \varepsilon \rangle^2 \right), \quad (19)$$

where  $L$  is the pathlength (assuming  $L \gg l_{\varepsilon}$ ) and  $\sigma_{\varepsilon}$  is the standard deviation of the synchrotron emissivity.

The resulting dependence of  $l_{\varepsilon}$  on the integral scale of the magnetic field  $l_b = \pi/(2k_0)$ , obtained in Eq. (15), can be approximated as

$$l_{\varepsilon}/L \approx G^{-1} (4l_b/L)^{0.65}, \quad (20)$$

where the numerical factor  $G$  depends on the model parameters and the cross-correlation coefficient  $C$ . The contours of  $G$  in the  $(\delta_n, C)$ -plane are shown in Fig. 7;  $G = 9$ –10 are representative values for  $\delta_b > 2$ –3. The resulting values of  $N = L/(2l_{\varepsilon})$  are used below to compare the synchrotron fluctuations obtained from observations in Section 4 with the model of Section 5.

### 6.3 Correlation between cosmic rays and magnetic fields

The relative intensity of synchrotron fluctuations is sensitive to the number  $N$  of correlations cells of synchrotron emissivity within the beam (or along the line of sight in case of a pencil beam). When comparing the theoretical model with observations, we adopt  $L = 1$  kpc for the pathlength in the Milky Way,  $l_{b_i} = 50$  pc for the correlation length of magnetic field,  $\delta_b = 3$  (the asymptotic limit  $\delta_b \gg 1$  is quite accurate in this case), and explore the range  $-1 \leq C \leq 1$  for the cross-correlation coefficient between cosmic-ray and magnetic fluctuations. For  $l_b/L = 0.05$  and  $G \approx 9$  (see Fig. 7), we have  $l_{\varepsilon} \approx 40$  pc and  $N = L/(2l_{\varepsilon}) \simeq 10$ ; we also discuss the effect of larger values of  $N$ .

Figure 8 shows the dependence of  $\delta_I = \sigma_I/I_0$  on the cross-correlation coefficient  $C$  for various values of the parameters  $\delta_b$  and  $\delta_n$ . The calculations are based on 100 realizations of  $\mathbf{B}$ , so the statistical errors of the mean values shown are negligible.

As can be seen from the upper panel of Fig. 8, the relative magnitude of synchrotron fluctuations,  $\delta_I \sqrt{N} > 0.7$ , obtained for  $\delta_b \geq 1$  and  $\delta_n = 0.5$ , is stronger than what is observed in the Milky Way,  $\delta_I \sqrt{N} = 0.3$ –0.6 assuming  $N = 10$ . If  $N = 20$ , the conservative observational estimate  $\delta_I = 0.1$ –0.2 translates into  $\delta_I \sqrt{N} = 0.4$ –0.9, implying  $C \lesssim -0.6$  at the upper end of this range. Thus,  $\delta_n < 0.5$  seems to be justified, unless  $N$  is significantly larger than 10 or, otherwise,  $\delta_b < 1$  (which is highly implausible). Since the estimate  $\delta_I = 0.1$ –0.2 has been obtained for high Galactic latitudes, the path length is unlikely to be much longer than 1 kpc, and the correlation length of the synchrotron fluctuations can hardly be much shorter than about 50 pc. Thus, excluding the case

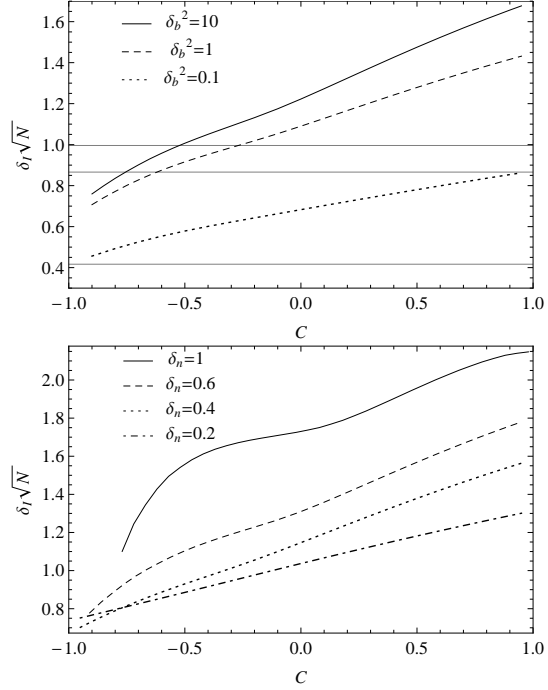


**Figure 8.** Relative fluctuations of the synchrotron intensity in synthetic radio maps of Section 6.1 versus the cross-correlation coefficient between  $B^2$  and  $n_{\text{cr}}$  for various choices of the model parameters. Top panel: a selection of  $\delta_b$  values for fixed  $\delta_n = 0.5$  (solid:  $\delta_b^2 = 10$ ; dashed: 1; dotted: 0.1). Grey horizontal lines correspond to uniformly distributed cosmic rays,  $\delta_n = 0$ , for the same values of  $\delta_b$  (with  $\delta_I$  decreasing with  $\delta_b$ ). Lower panel: various values of  $\delta_n$  for  $\delta_b^2 = 10$  ( $\delta_n = 1$ , solid; 0.6, dashed; 0.4, dotted; 0.2, dash-dotted).

of simultaneously large  $L$  and small  $l_{\varepsilon}$ , we conclude that the distribution of cosmic ray electrons is unlikely to have any significant variations at scales of order 50–100 pc.

The lower panel in Fig. 8, where a range of values of  $\delta_n$  are used with  $\delta_b^2 = 10$ , suggests that any positive correlation between cosmic rays and magnetic fields is only compatible with the observational estimate  $\delta_I \sqrt{N} = 0.3$ –0.6 (for  $N = 10$ ) if  $\delta_n < 0.2$ . In fact, an upper limit  $\delta_I \sqrt{N} = 0.9$  (for  $N = 20$ ) might be achieved for  $n_{\text{cr}} = \text{const}$ . The values of  $\delta_I \sqrt{N}$  in this case are shown with grey horizontal lines in the upper panel: for example,  $\delta_I \sqrt{N} = 1$  is compatible with  $\delta_b^2 = 10$ . However, the lower values of synchrotron fluctuations in the Milky Way in the range  $\delta_I \sqrt{N} = 0.3$ –0.9 for  $N = 10$ –20 can be compatible with the presence of fluctuations in cosmic ray density mildly anticorrelated with those in magnetic field. It is difficult to be precise here, but  $\delta_n < 0.2$  and  $C < -0.5$  seems to be an acceptable combination of parameters.

## 7 PROPAGATION OF COSMIC RAYS AND EQUIPARTITION WITH MAGNETIC FIELDS

To illustrate the relation between cosmic rays and magnetic fields, consider a simple model of cosmic ray propagation near a magnetic flux tube. The number density of cosmic rays  $n_{\text{cr}}$  (or their energy density  $\epsilon_{\text{cr}}$ ) is assumed to obey diffusion equation with the source  $Q$  and diffusivity  $D$  depending on magnetic field (Parker 1969; Kuznetsov & Ptuskin 1983; Schlickeiser & Lerche 1985). Consider a steady state of a one-dimensional system with  $Q = \text{const}$ . Magnetic field is assumed to have a statistically uniform fluc-

tuating component,  $\overline{b^2} = \sigma_b^2 = \text{const}$ , whereas the mean field is confined to a Gaussian slab of half-thickness  $L$  symmetric with respect to  $x = 0$ :  $B_y = B_0 \exp[-x^2/(2d^2)]$ ,  $B_x = B_z = 0$ . The cosmic ray diffusivity is assumed to depend on the relative strength of magnetic fluctuations,  $D = D_0 \sigma_b^2 / B_y^2$ . The resulting steady-state diffusion equation

$$\frac{d}{dx} D \frac{d}{dx} n_{\text{cr}} + Q = 0,$$

can easily be solved with the boundary conditions

$$\frac{dn_{\text{cr}}}{dx}(0) = 0, \quad n_{\text{cr}}|_{|x| \rightarrow \infty} = 0,$$

to yield

$$n_{\text{cr}} = \frac{QB_0^2 d^2}{2D_0 \sigma_b^2} e^{-x^2/d^2}. \quad (21)$$

The total number (and energy) of cosmic rays remains finite despite the uniform distribution of their sources,  $Q = \text{const}$ , because  $D \rightarrow \infty$  as  $|x| \rightarrow \infty$  in this illustrative model.

This simple solution shows that, near a magnetic flux tube in a statistically homogeneous random magnetic field, cosmic rays concentrate where the total magnetic field is stronger because their diffusivity is smaller there. In this example, the spatial distributions of cosmic rays and magnetic field are tightly correlated.

Another type of arguments relating cosmic ray energy density to parameters of the interstellar medium was suggested by Padoan & Scalo (2005). If both the magnetic flux and the cosmic ray flux are conserved,  $BS = \text{const}$  and  $n_{\text{cr}}US = \text{const}$  (where  $B$  is the magnetic field strength and  $S$  is the area within a fluid contour, and  $U$  is the cosmic ray streaming velocity), one obtains  $n_{\text{cr}}U/B = \text{const}$ , which yields  $n_{\text{cr}} \propto n^{1/2}$ , given that  $U = V_A \propto Bn^{-1/2}$ , with  $n$  the gas number density and  $V_A$  the Alfvén speed. Thus, cosmic ray energy density is independent of magnetic field strength and scales with thermal gas density. This result relies on the fact that the streaming velocity of the cosmic rays is proportional to the Alfvén speed. If, instead,  $U = V$ , with  $V$  the gas speed, we obtain  $n_{\text{cr}} \propto B$  from these arguments. No clear scaling of  $\epsilon_{\text{cr}}$  with magnetic field was observed in the simulations of Snodin et al. (2006) who use the gas velocity for  $U$ .

Assumption of the detailed, point-wise (local) equipartition between cosmic rays and magnetic fields is dubious also because these two quantities have vastly different diffusivities, and therefore cannot be similarly distributed in space. Magnetic filaments and sheets produced by the small-scale dynamo in the diffuse warm gas can have scales as small as a few parsecs (Shukurov 2007), and the strength of this turbulent magnetic field can be about  $5 \mu\text{G}$ . The large-scale magnetic field varies over scales of order 1 kpc, consistent with the turbulent diffusivity of  $10^{26} \text{ cm}^2 \text{ s}^{-1}$  and time scale  $5 \times 10^8 \text{ yr}$ . The diffusive length scale of cosmic rays, based on the diffusivity of  $D \simeq 10^{28} \text{ cm}^2 \text{ s}^{-1}$  and the confinement time in the disc,  $\tau \simeq 10^7 \text{ yr}$ , is about  $(2D\tau)^{1/2} \simeq 1 \text{ kpc}$ , similar to that of the large-scale magnetic field. On these grounds, is not impossible that the energy densities of cosmic rays and the *large-scale* magnetic field vary at similar scales, but this would be very implausible for the total magnetic field. Then equipartition arguments may be better applicable to observations of external galaxies, where the linear resolution is not better than a few hundred parsecs, than to the case of the Milky Way.

## 8 DISCUSSION

The general picture emerging from our results is where cosmic rays and magnetic fields are slightly anticorrelated at the relatively small, sub-kiloparsec scales explored here ( $n_{\text{cr}} = \text{const}$  is also a viable possibility). Such an anticorrelation can result from the statistical pressure equilibrium in the ISM, where cosmic rays and magnetic fields make similar contributions to the total pressure. An additional effect leading to an anticorrelation is the increase in the synchrotron losses of relativistic electrons in stronger magnetic field. However, equipartition between cosmic rays and magnetic field cannot be excluded at larger scales of order and larger than 1 kpc. Hoernes et al. (1998) indirectly make a similar conclusion concerning loss of equipartition at small scales from their analysis of the radio–far-infrared correlation in M31.

Since magnetic fields and cosmic rays have vastly different diffusivities, and therefore, must vary at very different scales, any strong correlation between them can hardly be expected at scales smaller than 1 kpc. Correlated (or rather anticorrelated) fluctuations can, however, arise from such secondary processes as the adjustment to pressure equilibrium, etc.

Our arguments and conclusions are based on observations and modelling of synchrotron emission, a tracer of the electron component of cosmic rays. Thus, our conclusions strictly apply to the cosmic ray electrons. However, the only significant difference between the behaviour of electrons and protons in this context is that the former experience by far stronger energy losses due to synchrotron emission and inverse Compton scattering off the relic microwave photons. The energy loss time scale  $\simeq 4 \times 10^8 \text{ yr} (E/1 \text{ GeV})^{-1}$  in magnetic field of  $5 \mu\text{G}$  in strength, for particles emitting at wavelengths larger than 1 cm, is much longer than the confinement time  $10^7 \text{ yr}$ , so the energy losses are negligible unless the local magnetic field is unusually strong. Therefore, we extend our conclusions derived from analysis of synchrotron fluctuations to cosmic rays as a whole. Moreover, energy losses can only make the distribution of the electrons more inhomogeneous than that of the protons, so that our conclusions are robust with respect to this caveat.

Our results can significantly change the interpretation of high-resolution radio observations of the Milky Way and spiral galaxies. Present interpretations, aimed at estimating the strength and geometry of interstellar magnetic fields, rely heavily on the assumption of local equipartition between cosmic rays and magnetic fields, at a scale corresponding to the resolution of the observations. This assumption is acceptable if the resolution is not finer than the diffusion length of the cosmic rays, about 1 kpc. However, this assumption is questionable when applied to observations at higher resolution. We can suggest a different procedure to interpret such observations. The original radio maps should first be smoothed to the scale of the cosmic ray distribution, 1 kpc, where the equipartition assumption *may* apply, and the distribution of cosmic rays can be deduced from the smoothed data. After that, this distribution of cosmic rays can be used to deduce magnetic field distribution from the data at the original resolution. Since a larger part of the synchrotron fluctuations observed will be attributed to magnetic fields, it is clear that this procedure will result in a more inhomogeneous magnetic field than that arising from the assumption of local equipartition so often used now.

## ACKNOWLEDGMENTS

We are grateful to the Royal Society and Newcastle University for financial support. At various stages, this work was supported

by the Leverhulme Trust under Research Grant RPG-097, the Royal Society, and by the National Science Foundation under Grant NSF PHY05-51164. RS acknowledges support from the grant YD-4471.2011.1 of the Council of the President of the Russian Federation.

## APPENDIX A: THE CROSS-CORRELATION COEFFICIENT OF $B^2$ AND $n_{\text{cr}}$

Here we derive analytical expressions for the mean value and the standard deviation of synchrotron intensity for the model of partially correlated magnetic fields and cosmic rays introduced in Section 5. We assume that each Cartesian vectorial component of the random magnetic field  $\mathbf{b}$  is a Gaussian random variable with zero mean value,  $\overline{b_i} = 0$ , and that the vector field is isotropic,

$$\overline{b_i^2} = \frac{1}{3} \overline{b^2} = \frac{1}{3} \sigma_b^2, \quad (\text{A1})$$

where  $i = x, y, z$  and bar denotes ensemble averaging. Then

$$\overline{b_i^{2k}} = \frac{(2k)!}{2^k k!} \sigma_b^{2k}, \quad \overline{b_i^{2k+1}} = 0. \quad (\text{A2})$$

The cross-correlation coefficient of  $n_{\text{cr}}$  and  $B^2$  is defined as

$$C(B^2, n_{\text{cr}}) = \frac{\overline{n_{\text{cr}} B^2} - \overline{n_{\text{cr}}} \overline{B^2}}{\sigma_{n_{\text{cr}}} \sigma_{B^2}}.$$

Given Eq. (17), it can be shown that

$$\overline{n_{\text{cr}} B^2} = \alpha \sigma_{B^2}^2 + n_0 \overline{B^2} \quad \text{and} \quad \sigma_n^2 = \alpha^2 \sigma_{B^2}^2 + \beta^2 \sigma_{B^2}^2.$$

Then  $C(B^2, n_{\text{cr}})$  is equal to a given value  $C$ ,

$$\frac{\alpha}{\sqrt{\alpha^2 \sigma_{B^2}^2 + \beta^2 \sigma_{B^2}^2}} = C,$$

provided

$$\alpha = \frac{C}{\sigma_{B^2}} \quad \text{and} \quad \beta = \frac{\sqrt{1 - C^2}}{\sigma_{B^2}}.$$

For given  $n_{\text{cr}}$  and  $\mathbf{B}$ , the mean value and the standard deviation of the synchrotron intensity can be calculated using the following relations, obtained using Eqs (A1) and (A2):

$$\begin{aligned} \overline{B_{\perp}^4} &= B_{0\perp}^4 + \frac{8}{3} B_{0\perp}^2 \sigma_b^2 + \frac{8}{9} \sigma_b^4, \\ \overline{B^2 B_{\perp}^4} &= B_{0\perp}^4 B_{0\parallel}^2 + \frac{8}{3} B_{0\perp}^2 \sigma_b^2 B_z^2 + \frac{8}{9} \sigma_b^4 B_{0\parallel}^2 \\ &\quad + B_{0\perp}^6 + \frac{19}{3} B_{0\perp}^4 \sigma_b^2 + \frac{80}{9} B_{0\perp}^2 \sigma_b^4 + \frac{56}{27} \sigma_b^6, \\ \overline{B^4 B_{\perp}^4} &= 2 B_{0\perp}^6 B_{0\parallel}^2 + 14 B_{0\perp}^4 \sigma_b^2 B_{0\parallel}^2 + B_{0\perp}^4 B_{0\parallel}^4 \\ &\quad + \frac{64}{3} B_{0\perp}^2 \sigma_b^4 B_{0\parallel}^2 + \frac{8}{3} B_{0\perp}^2 \sigma_b^2 B_{0\parallel}^4 \\ &\quad + \frac{16}{3} \sigma_b^6 B_{0\parallel}^2 + \frac{8}{9} \sigma_b^4 B_{0\parallel}^4 + B_{0\perp}^8 + \frac{34}{3} B_{0\perp}^6 \sigma_b^2 \\ &\quad + \frac{109}{3} B_{0\perp}^4 \sigma_b^4 + \frac{104}{3} B_{0\perp}^2 \sigma_b^6 + \frac{56}{9} \sigma_b^8. \end{aligned}$$

From Eq. (6), we have  $I = L \langle \varepsilon \rangle_L$ , where angular brackets denote spatial averaging, with subscript indicating the averaging region:  $L$  for the line of sight,  $S$  for the area and  $V$  for the volume averaging. This leads to  $I_0 = \langle I \rangle_S = L \langle \varepsilon \rangle_V = N l_{\varepsilon} \overline{\varepsilon}$  provided that  $N = L/(2l_{\varepsilon}) \gg 1$ . Finally, we obtain, from  $I_0 = L n_{\text{cr}} \overline{B^2}$  and  $\sigma_I^2 = L l_{\varepsilon} (\overline{\varepsilon^2} - \overline{\varepsilon}^2)$ :

$$I_0 = \frac{N l_{\varepsilon}}{9} [4\alpha \delta_n \sigma_b^4 + 6\sigma_b^2 + 3(4\alpha \delta_n \sigma_b^2 + 3) B_{0\perp}^2], \quad (\text{A3})$$

and

$$\begin{aligned} \sigma_I^2 &= \frac{N l_{\varepsilon}^2}{81} \left\{ 224\alpha^2 \delta_n^2 \sigma_b^8 + 144\alpha \delta_n (9\alpha \delta_n B_{0\perp}^2 + 1) \sigma_b^6 \right. \\ &\quad + 18 [51\alpha^2 \delta_n^2 B_{0\perp}^4 + 36\alpha \delta_n B_{0\perp}^2 - 4\delta_n^2 (C^2 - 1) + 2] \sigma_b^4 \\ &\quad + 12\alpha^2 \delta_n^2 (9B_{0\perp}^4 + 24\sigma_b^2 B_{0\perp}^2 + 8\sigma_b^4) B_{0\parallel}^2 \sigma_b^2 \\ &\quad + 108 [(\alpha \delta_n B_{0\perp}^2 + 1)^2 - 2\delta_n^2 (C^2 - 1)] B_{0\perp}^2 \sigma_b^2 \\ &\quad \left. - 81\delta_n^2 (C^2 - 1) B_{0\perp}^4 \right\}. \end{aligned} \quad (\text{A4})$$

## REFERENCES

- Arbutina B., Urošević D., Andjelić M. M., Pavlović M. Z., Vukotić B., 2012, *ApJ*, 746, 79
- Arshakian T. G., Stepanov R., Beck R., Krause M., Sokoloff D., 2011, *Astron. Nachr.* 332, 524
- Banday A. J., Giller M., Wolfendale A. W., 1991a, in *The 22nd International Cosmic Ray Conference*, Vol. 2, p. 736
- Banday A. J., Wolfendale A. W., Giler M., Szabelska B., Szabelski J., 1991b, *ApJ*, 375, 432
- Beck R., 2007, *A&A*, 470, 539
- Beck R., Brandenburg A., Moss D., Shukurov A., Sokoloff D., 1996, *ARAA*, 34, 155
- Beck R., Fletcher A., Shukurov A., Snodin A., Sokoloff D. D., Ehle M., Moss D., Shoutenkov V., 2005, *A&A*, 444, 739
- Beck R., Krause M., 2005, *Astron. Nachr.*, 326, 414
- Berezinskii V. S., Bulanov S. V., Dogel V. A., Ginzburg V. L., Ptuskin V. S., 1990, *Astrophysics of Cosmic Rays*. North-Holland, Amsterdam
- Bridle A. H., 1967, *MNRAS*, 136, 219
- Burbidge G. R., 1956a, *ApJ*, 124, 416
- Burbidge G. R., 1956b, *ApJ*, 123, 178
- Burn B. J., 1966, *MNRAS*, 133, 67
- Carilli C. L., Taylor G. B., 2002, *ARAA*, 40, 319
- Casse F., Lemoine M., Pelletier G., 2002, *Phys. Rev. D*, 65, 023002
- Chi X., Wolfendale A. W., 1993, *Nat*, 362, 610
- Christensson M., Hindmarsh M., Brandenburg A., 2001, *Phys. Rev. E*, 64, 056405
- Chyży K. T., 2008, *A&A*, 482, 755
- Dagkesamanskii R. D., Shutenkov V. R., 1987, *Sov. Astron. Lett.*, 13, 73
- Fletcher A., Beck R., Shukurov A., Berkhuijsen E. M., Horellou C., 2011, *MNRAS*, 412, 2396
- Galtier S., Nazarenko S. V., Newell A. C., Pouquet A., 2000, *J. Plasma Phys.*, 63, 447
- Getmantsev G. G., 1959, *Sov. Astron.*, 3, 415
- Giacalone J., Jokipii J. R., 1999, *ApJ*, 520, 204
- Haslam C. G. T., Salter C. J., Stoffel H., Wilson W. E., 1982, *A&AS*, 47, 1
- Hoernes P., Berkhuijsen E. M., Xu C., 1998, *A&A*, 334, 57
- Kuznetsov V. D., Ptuskin V. S., 1983, *Ap&SS*, 94, 5
- La Porta L., Burigana C., Reich W., Reich P., 2008, *A&A*, 479, 641
- Laing R. A., 1980, *MNRAS*, 193, 439
- Lithwick Y., Goldreich P., Sridhar S., 2007, *ApJ*, 655, 269
- Longair M. S., 1994, *High energy astrophysics. Vol.2: Stars, the galaxy and the interstellar medium*. Cambridge: Cambridge University Press, 2nd ed.
- Malik N. A., Vassilicos J. C., 1999, *Phys. Fluids*, 11, 1572
- Mills B. Y., Slee O. B., 1957, *Austr. J. Phys.*, 10, 162

- Moss D., Stepanov R., Arshakian T. G., Beck R., Krause M., Sokoloff D., 2012, *A&A*, 537, A68
- Ohno H., Shibata S., 1993, *MNRAS*, 262, 953
- Oppermann N., Jankewitz H., Robbers G., Enßlin T. A., 2011, *A&A*, 530, A89
- Orienti M., Dallacasa D., 2008, *A&A*, 487, 885
- Padoan P., Scalo J., 2005, *ApJ*, 624, L97
- Parker E. N., 1966, *ApJ*, 145, 811
- Parker E. N., 1969, *Space Sci. Rev.*, 9, 651
- Parker E. N., 1979, *Cosmical magnetic fields: Their origin and their activity*. Oxford, Clarendon Press,
- Pohl M., 1993, *A&A*, 279, L17
- Readhead A. C. S., 1994, *ApJ*, 426, 51
- Roger R. S., Costain C. H., Landecker T. L., Swerdlyk C. M., 1999, *A&AS*, 137, 7
- Rogstad D. H., Wright M. C. H., Lockhart I. A., 1976, *ApJ*, 204, 703
- Ruzmaikin A. A., Shukurov A. M., Sokoloff D. D., 1988, *Magnetic Fields of Galaxies*. Kluwer, Dordrecht
- Scheuer P. A. G., Williams P. J. S., 1968, *ARAA*, 6, 321
- Schlickeiser R., Lerche I., 1985, *A&A*, 151, 151
- Scott M. A., Readhead A. C. S., 1977, *MNRAS*, 180, 539
- Shukurov A., 2007, in *Mathematical Aspects of Natural Dynamos*, Dormy E., Soward A. M., eds., London, Chapman and Hall/CRC, pp. 313–359
- Sligh V. I., 1963, *Nat*, 199, 682
- Snodin A. P., Brandenburg A., Mee A. J., Shukurov A., 2006, *MNRAS*, 373, 643
- Sokoloff D. D., Bykov A. A., Shukurov A., Berkhuijsen E. M., Beck R., Poetz A. D., 1998, *MNRAS*, 299, 189
- Stepanov R., Arshakian T. G., Beck R., Frick P., Krause M., 2008, *A&A*, 480, 45
- Stepanov R., Fletcher A., Shukurov A., Beck R., La Porta L., Tabatabaei F. S., 2009, in *IAU Symposium*, Vol. 259, pp. 93–94
- Stil J. M., Krause M., Beck R., Taylor A. R., 2009, *ApJ*, 693, 1392
- Sveshnikov A. A., 1966, *Applied Methods of the Theory of Random Functions*. Elsevier, Amsterdam
- Tabatabaei F. S., Beck R., Krügel E., Krause M., Berkhuijsen E. M., Gordon K. D., Menten K. M., 2007b, *A&A*, 475, 133
- Tabatabaei F. S., Krause M., Beck R., 2007a, *A&A*, 472, 785
- Tabatabaei F. S., Krause M., Fletcher A., Beck R., 2008, *A&A*, 490, 1005
- Volegova A. A., Stepanov R. A., 2010, *JETP Lett.*, 90, 637
- Wilkin S. L., Barengi C. F., Shukurov A., 2007, *Phys. Rev. Lett.*, 99, 134501
- Williams P. J. S., 1963, *Nat*, 200, 56